Utilization of Granular Activated Carbon for Sustainable Environmental Contaminants Remediation

YOGITA K. MESHRAM[1]*, RAM U. KHOPE[2] and RESHAL A. DESHMUKH[3]

[1,2,3]Department of Chemistry, S.S.E.S Amt's Science College, Congressnagar, Nagpur, (M.S), India.
*Corresponding author E-mail: meshramyogita249@gmail.com

ABSTRACT

An environment eco-friendly adsorbents such as filtrasorb-816 and filtrasorb-820 were used in this work. For the evaluation of the adsorption of manganese from the aqueous phase, granular activated carbons were used in conjunction with organic ligands such as 3,5-Dinitrobenzoic acid. The phenomenon of adsorption characteristics of manganese in an aqueous phase was studied at a constant temperature of 25 ±1°C and pH 5. Granular activated carbons were characterized by SEM analysis. Experimental data were tested by using Pseudo-first and Pseudo-second-order kinetic models. From the results, it was investigated that Pesudo-second-order data is more favorable than the pseudo-first-order for this system. The Langmuir, Freundlich, and Temkin isotherms models were used to describe the equilibrium characteristics of adsorption of Mn^{2+} onto activated carbon but the R^2 value of the Langmuir isotherm model was higher than other isotherms and hence it is the best fit. From this study, it was found that F-820 has more adsorption capacity to scavenge Mn^{2+} than F-816 from aqueous phase.

Keywords: Granular activated carbon, Manganese, Isotherm, Adsorption, Heavy metals.

INTRODUCTION

Water is a crucial advent for human beings and is used in many sectors. Rapid and unorganized urban and industrial developments have contributed to various environmental issues. The water resources continue to be contaminated with run-off water from agriculture fields containing pesticides, fertilizers, the industrial effluents, raising serious health and environmental concerns. The improper disposal and management of industrial and municipal wastewater are major sources of water pollution. Polluted water contains toxic metals, inorganic chemicals, and colored reagents creating a significant threat to public health.

Industries such as electroplating, leather, and textiles release substantial amounts of heavy metals, including arsenic, manganese, chromium, cobalt, lead, and nickel, contributing significantly to water pollution. Heavy metals highly reactive and non-degradable which may be deposited on the surface and water

resources, posing immense dangers to all forms of life and the environment[1,2]. The excess level of manganese in the water causes several detrimental consequences and can damage multiple organ of human[3]. As well as manganese deficiencies causes wide range of clinical complications, including migraines, fibromyalgia, arrhythmia[4]. Consequently, the removal of heavy metals from wastewater is a challenging task that demands continuous monitoring and attention. Heavy metals, accumulate in the environment, emphasizing the urgency of their removal from wastewater before discharge. Several treatment methods, such as chemical reduction, electro-coagulation, membrane adsorption[5], ion exchange[6,7], precipitation, membrane separation[8], and adsorption are available to lower the Mn(II) ion concentration from industrial wastewater[9,10]. To prevent future adverse consequences on both human beings and the environment, these hazardous metals must be effectively removed from wastewater. However, the effective method for the treatment of heavy metals is the adsorption technique and the specific properties of adsorbents elevate the adsorption process. The appropriate selection of adsorbents is crucial, focusing on functional groups, high surface area, porosity, and polarity of adsorbents. Adsorption has proven to be more efficient and cost-effective for heavy metal removal compared to other methods. Its fundamental advantage lies in its economic viability, making it a low-cost approach for heavy metal removal. Another significant benefit of the adsorption process is its ability to be regenerated, allowing for the repeated use of adsorbents[11,12]. Both commercial and conventional adsorbents have applications in scavenging heavy metals from aqueous phases[13,14].

Various low cost adsorbents were used by different researchers for the removal of heavy metals from aqueous phase[15,16]. Heavy metal pollution remains a pressing concern, and adsorption offers a powerful solution. This method not only effectively remediates heavy metals from wastewater but also demonstrates a minimal environmental impact. This makes it a green technology that significantly enhances the wastewater treatment process.[17-20]

MATERIAL AND METHOD

All chemicals of analytical grade were utilized. Initially, a requisite amount of $MnSO_4$ was dissolved in 1 liter of distilled water to prepare a stock solution of Mn^{2+} ions. Different grades of carbon were initially sized using a siever, resulting in particles ranging from 840μ to 1400μ mesh size. Subsequently, activated carbon particles F-816 and F-820 were thoroughly washed with boiled distilled water repeatedly, till a clear leachate was obtained. The washed carbon particles were collected and dried at a temperature of 100-110°C in an oven and then stored in desiccator till further use.

3,5-Dintrobenzoic acid was chosen as the ligand and then it is recrystallized by conventional method. The purity of 3,5-Dinitrobenzoic acid an essential component of the experiment, was confirmed by determining its melting point using Thiele's apparatus. The experimental melting point of 206°C was in close agreement with the literature value of 207°C, indicating its purity[21].

For determining adsorption isotherm, 200 mL solution containing a specific concentration of 3,5-Dinitrobenzoic acid and 0.5 g dried granular activated carbon were taken in a shaking bottle. The mixture was shaken for 5 h using a mechanical shaker (Remi Model, No. R.S.24). After that, the solution was filtered out, and the carbon was properly washed with distilled water multiple times. Then, 200 ml Mn^{2+} ion solution of pH 5 and washed carbon were transferred into the shaking bottle. The resulting mixture was shaken at a constant temperature of 25±1°C for 5 hours. The Mn^{2+} ions concentration, both before and after adsorption, was determined in mg/L by measuring absorbances using a spectrophotometer. The experimental data were analyzed using a calibration curve, ensuring accurate quantification. The graph was drawn by using the values of absorbance and concentrations of different standard solutions of Mn^{2+}. To guarantee the reliability of the results, the experiments were repeatedly done to ensure consistency and reproducibility.
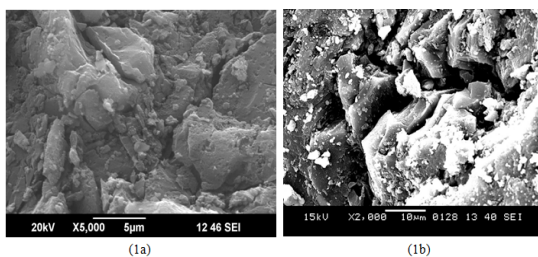
RESULT AND DISCUSSION

Fig. 1a. Scanning electron Micrograph of F-816 before adsorption and 1b-after adsorption of Mn²⁺, System: F-816_3,5-Dinitrobenzoicacid_ Mn²⁺
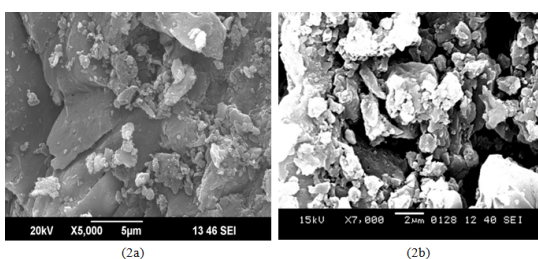

Fig. 2a. Scanning electron micrograph of F-820 before adsorption and 2b-after adsorption of Mn²⁺, System: F-820_3,5-Dinitrobenzoic acid _Mn²⁺

Scanning electron micrographs were taken at various magnifications, displayed in Fig. 1a and 2a, revealing large cracks and uneven cavities on the surface of both Granular Activated Carbon (GAC) i.e. F-816 and F-820. These irregularities provide a substantial surface area, enhancing the metal adsorption capacity for Mn^{2+} ions. Changes in the adsorbent's surface morphology after adsorption are illustrated in Fig. 1b and Fig. 2b. It was noted that the previously uniform porosity of the adsorbent was disrupted due to the accumulation of Mn^{2+} ions on the carbon surface.

The Adsorption of Mn^{2+} ions on ligand-loaded GAC was investigated using batch adsorption studies. The concentration of Mn^{2+} ions was calculated by the following equation,

$$q_e = (C_0 - C_e) \times V/W$$

Where q_e = The concentration of Mn^{2+} on the ligand-loaded granular activated carbon, expressed in milligrams per millimole of ligand, the initial and equilibrium concentrations of Mn^{2+} ions i.e. C_o and C_e, in milligrams per liter respectively. The variables V and W represent the volume of the solution in liters and the weight of the adsorbent in grams, respectively. The equilibrium isotherms for the ligand-loaded granular activated carbon were obtained by plotting the graph of q_e (the amount of adsorbed Mn^{2+} per millimole of ligand) against C_e (the equilibrium concentration of Mn^{2+} ions). The results of these plots are illustrated in Fig. 3 and Fig. 4.
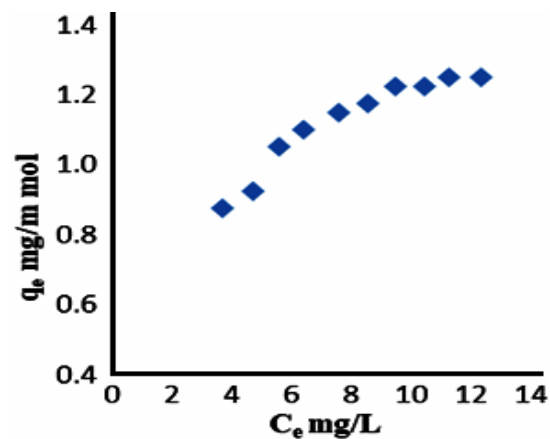

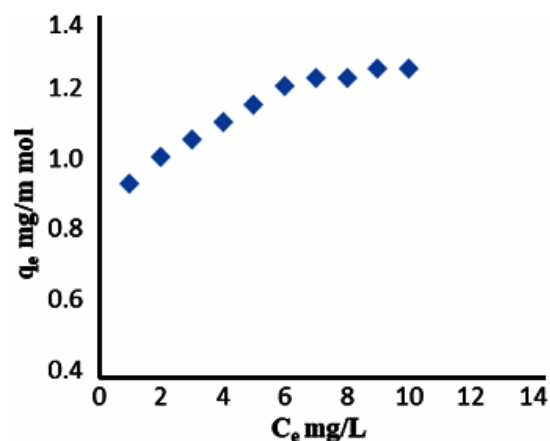**Fig. 3. Equilibrium Isotherm, System- F-816_3,5-Dinitrobenzoic acid_Mn²⁺**

Fig. 4. Equilibrium isotherm, System-F-820_3,5-Dinitrobenzoic acid_ Mn²⁺

Langmuir, Freundlich, and Temkin models were used in an attempt to fit the equilibrium isotherm data on both systems i.e. F 816-3,5-Dinitrobenzoic acid+Mn²⁺ and F-820-3,5-Dinitrobenzoic acid+Mn²⁺.

In the first, the linearized form of the Langmuir equation is expressed by the following equation.[22]

$$\frac{1}{q_e} = \frac{1}{bQ^o} \times \frac{1}{C_e} + \frac{1}{Q^o}$$

The Langmuir constant, denoted as b, Q⁰

represents the amount adsorbed per unit weight of activated carbon forming a complex monolayer on the activated carbon.

The linear graphs of $1/q_e$ verses $1/C_e$ in Fig. 5 and 7 demonstrate the applicability of the Langmuir model. All the constants i.e. the Langmuir constant b and Q^0 were determined from the slope and intercept of the Langmuir isotherm, respectively given in Table 1. The Langmuir equation and corresponding regression coefficients are shown in Table 2.

The second one is the Freundlich model and equation[23] is represented as

$$q_e = K_f C_e^{1/n}$$

Above equation may be linearized as

$$\log q_e = \log k_f + 1/n \, \log C_e$$

Figure 6 and Fig. 8 show consistent linear plots of log C_e versus log q_e which demonstrate the validity of the Freundlich equation across a range of concentrations. The Freundlich constants, 1/n and K_f, were calculated from the slope and intercept of the Freundlich equation, respectively. These Freundlich constants have been reported in Table 1, and the corresponding equation along with the regression coefficients are presented in Table 2.

Third one is the Temkin model[24] which is represented by the following equation

$$q_e = \frac{RT}{b} \times \ln(K_T C_e)$$

The linearized form of the above equation can be expressed as

$$q_e = B_T \ln K_T + B_T \ln C_e$$

$$B_T = R_T/b$$

Where B_T is the Temkin constant associated with the heat of adsorption (in kJ/mol), The variation of adsorption energy b (kJ/mol), R is the Universal gas constant (8.314 J/mol·K), T is the absolute temperature (in K), and KT is the Temkin isotherm constant (in L/mg). The Temkin isotherm posits that

the heat of adsorption decreases linearly due to interactions between the adsorbent and adsorbate molecules. It provides insight into the adsorption potential of the adsorbent for the adsorbate. The Temkin constants, B_T and K_T, for Mn^{2+} ions were determined by plotting $\ln(C_e)$ against q_e. The resulting linear plots over a concentration range allowed the calculation of Temkin constants, which are presented in Table 1. The R^2 values indicated a partial fit of the data to the Temkin adsorption isotherm for both systems: F-816-3,5-Dinitrobenzoic acid+Mn^{2+} and F-820-3,5-Dinitrobenzoic acid+Mn^{2+}. The adsorption equilibrium data in this study were assessed using Langmuir, Freundlich, and Temkin isotherms. Fig. 5 to 10 depict the plots for the Langmuir, Freundlich, and Temkin isotherms, respectively. The correlation factor $R^2=1$ suggests that the Langmuir model provides a more accurate depiction of the adsorption process compared to the Freundlich and Temkin models.
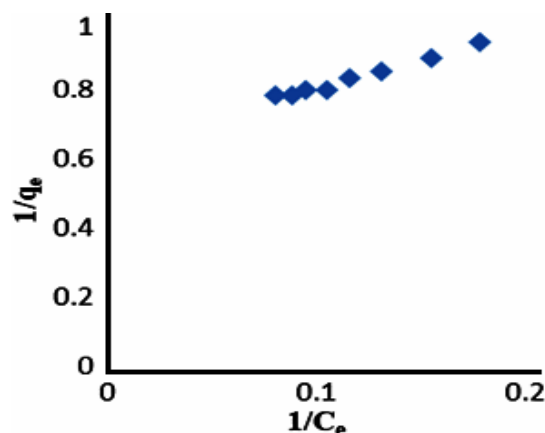

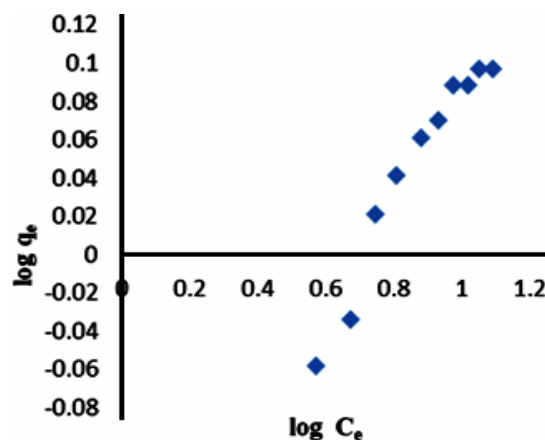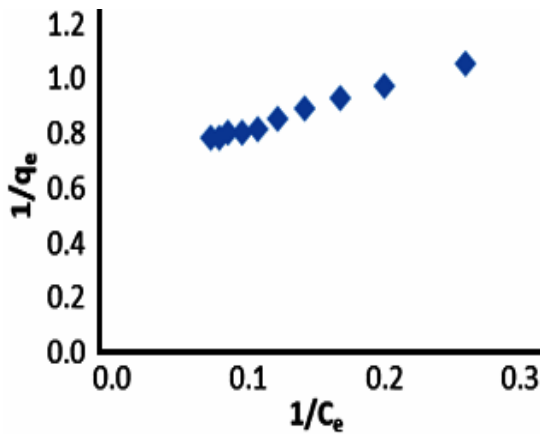**Fig. 5. Langmuir Adsorption Isotherm System-F-816_3,5-Dinitrobenzoic acid_Mn²⁺**

Fig. 6. Freundlich Adsorption Isotherm System-F-816_3,5-Dinitrobenzoic acid-Mn²⁺

Fig. 7. Langmuir Adsorption Isotherm
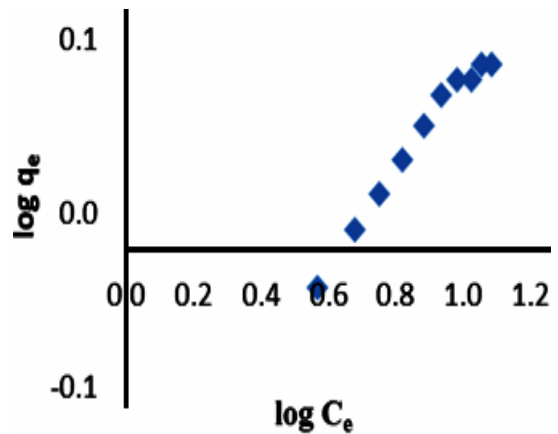**System-F-816_3,5-Dinitrobenzoic acid_Mn²⁺**

Fig. 8. Freundlich Adsorption Isotherm
System-F-820_3,5-Dinitrobenzoic acid-Mn²⁺
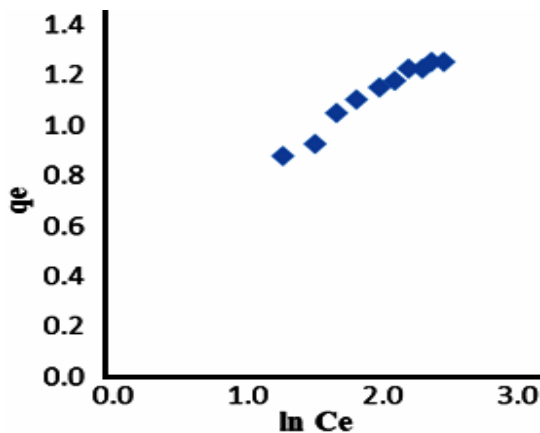

Fig. 9. Temkin Adsorption Isotherm
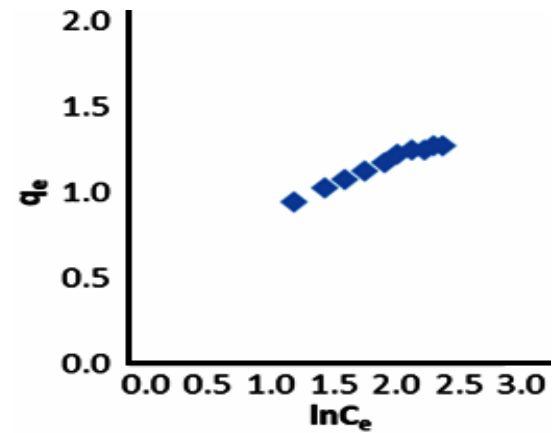**System-F-816_3,5-Dinitrobenzoic acid_Mn²⁺**

Fig. 10. Temkin Adsorption Isotherm
System-F-820_ 3,5-Dinitrobenzoic acid_Mn²⁺

Kinetics studies

To investigate the adsorption kinetics of Mn^{2+} on granular activated carbon (GAC), kinetic analyses employing Lagergren's pseudo-first-order and pseudo-second-order models were conducted. These analyses aid in understanding the rate of adsorption and identifying the rate-limiting step in the transport mechanism, essential for the design and modeling of the adsorption process.

The Lagergren pseudo-first-order model is described by the following linear equation:

$\ln(q_e - q_t) = \ln q_e - k1\, t$

Here, q_t is the amount of Manganese on the ligand absorbed on GAC (mg/mmol) at any time t, q_e is the amount of Manganese on the ligand absorbed on GAC at equilibrium (mg/mmol), and k1 is the rate constant of the pseudo-first-order adsorption process (h^{-1}). The values of k1 and qe are determined by plotting t versus $\ln(q_e - q_t)$. The metal uptake capacity at equilibrium and the rate constant for the pseudo-first-order model can be obtained from the slope and intercept of the plot. Table 3 presents the metal uptake capacity and rate constants for the pseudo-first-order model for different granular activated carbons. The experimental data for the F-816_3,5-Dinitrobenzoic acid_Mn²⁺ system and the F-820_3,5-Dinitrobenzoic acid_Mn²⁺ system are illustrated in Fig. 11 and Fig. 13, respectively.

The pseudo-second-order kinetics can be expressed in a linear form as follows:

$$\frac{t}{q_t} = \frac{1}{k_2 q_e^{2}} + \frac{1}{q_e}t$$

Here, k_2 is the rate constant of the pseudo-

second-order adsorption process. This equation allows for the determination of k_2 and q_e by plotting t/q_t against t.

The results of the pseudo-second-order

kinetics analysis provide further insights into the adsorption process i.e chemisorption and rate limiting step which contribute to a comprehensive understanding of system.
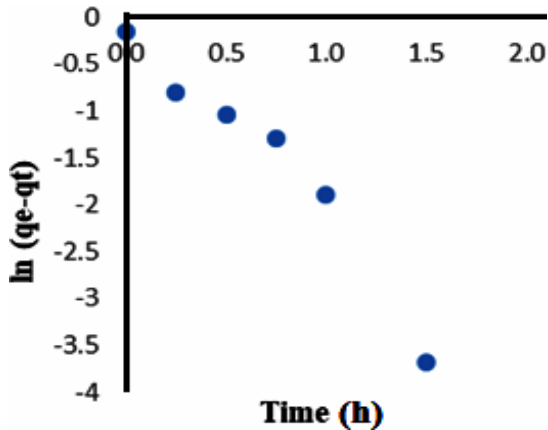

**Fig. 11. Pseudo first order model
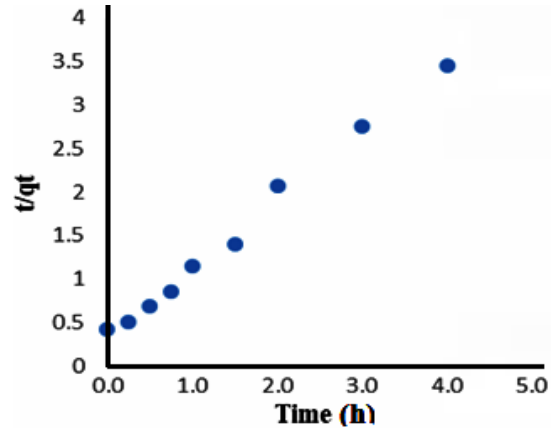System-F-816_3,5-Dinitrobenzoic acid_Mn²⁺**

**Fig. 12. Pseudo second order model
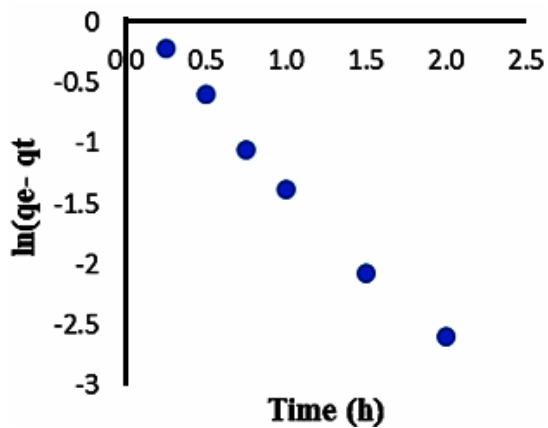System-F-816_3,5-Dinitrobenzoic acid_Mn²⁺**

**Fig. 13. Pseudo first order model System
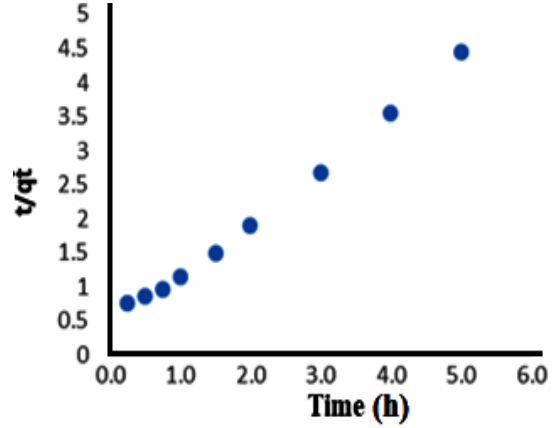F-820_3,5-Dinitrobenzoic acid_Mn²⁺**

**Fig. 14. Pseudo second order model System
F-820_3,5-Dinitrobenzoic acid_Mn²⁺**

Table 1: Constants for Langmuir, Freundlich and Temkin adsorption isotherm

S. No	System	Langmuir constant		Freundlich constant		Temkin constant		q_{max}(mg/m.mole
		Q_0	b	$1/n$	K_f	B_T	K_T	q_{max}
1	GAC- F 816-3,5-Dinitrobenzoic acid+Mn²⁺	1.5151	0.4091	0.310	0.5956	0.331	3.9165	1.2500
2	GAC-F-820 -3,5- Dinitrobenzoic acid+Mn²⁺	1.5337	0.4298	0.256	0.6886	0.228	7.4627	1.2750

Table 2: Isotherm equation and regression coefficient

S. No	Adsorption system	Equation	Reg. Coefficient	Types of isotherms
1	GAC-F-816-3,5-Dinitrobenzoic+Mn²⁺	y=1.6133x+0.6602	$R^2 = 0.9853$	Langmuir adsorption isotherm
2	GACF-820-3,5-Dinitrobenzoic acid+Mn²⁺	y=1.5176x+0.6526	$R^2 = 0.9925$	Langmuir adsorption isotherm
3	GAC-F-816-3,5-Dinitrobenzoic acid+Mn²⁺	y=0.3105x-0.2251	R= 0.9660	Freundlich adsorption isotherm
4	GACF-820-3,5-Dinitrobenzoic acid+Mn²⁺	y=0.2567x-0.1623	$R^2 = 0.9780$	Freundlich adsorption isotherm
5	GAC-F-816-3,5-Dinitrobenzoic acid+Mn²⁺	y=0.331+0.452	$R^2=0.9610$	Temkin adsorption isotherm
6	GAC-F-820-3,5-Dinitrobenzoic acid+Mn²⁺	y=0.288+0.579	$R^2 = 0.9830$	Temkin adsorption isotherm

Table 3: Parameters of Pseudo First Order and Second Order Kinetic Model and Regression Coefficients

S. No	System	Pseudo First Order				Pseudo Second Order			
		K_1 (h^{-1})	q_e cal. mg/mmol	q_e expt mg/mmol	R^2	K^2	q_e cal mg/mmol	q^e expt mg/mmol	R^2
1	F-816_3,5-Dinitrobezoic acid-Mn^{2+}	2.1721	0.9771	1.2500	0.9326	1.9105	1.2600	1.2500	0.9935
2	F-820_3,5-Dinitrobezoic acid-Mn^{2+}	1.3566	1.0232	1.2750	0.9884	1.5306	1.2717	1.2750	0.9947

CONCLUSION

The experiment revealed a notable difference in adsorption capacity between GAC-F-820 and GAC-F-816, with GAC-F-820 demonstrating significantly higher performance. Langmuir, Freundlich, and Temkin models were employed to analyze the adsorption data for Manganese, and the results indicated that the Langmuir model exhibited the best fit, supported by a higher R^2 value, signifying a robust correlation. Kinetic analysis revealed the success of the Pseudo-second-order model, as evidenced by a high correlation coefficient (R^2). These findings highlight the potential of coal-based adsorbents, specifically GAC modified with organic ligands, to advance technologies for removing heavy metal ions from polluted industrial effluents. In summary, the modified GAC surface proves effective in reducing the concentration of Manganese ions in both industrial wastewater and aqueous solutions. The study underscores the importance of considering cost-effectiveness and technical applicability when selecting adsorbents for crucial applications.

Conflict of interest

The authors declare no conflict of interest

REFERENCES

1. Charerntanyarak, L. *Water Science and Technology.*, **1999**, *39*(10),135-138.
2. Tanong, K.; TranLH, M.G.; Blais, J. F. *J. Clean. Prod.*, **2017**, *148*, 233-244.
3. Dey S.; Tripathy, B.; Santosh Kumar, M.; Das, A. P. *Environmental Chemistry and Ecotoxicology.*, **2023**, *5*, 55-61.
4. Razzaque, M. S., *Nutrients.*, **2018**, *10*(12), 1863.
5. Peng, H.; Guo, *J. Environmental Chemistry Letters.*, **2020**, 1-4.
6. Khulbe, K.C.; Matsuura,T., *Applied Water Science.*, **2018**, 8-19.
7. Abo-Farha, S. A.; Abdel-Aal, A.Y.; Ashour, I. A.; Garamon, S. E. *J. Hazard. Mater.*, **2009**, *169*, 190-194.
8. Alyuz, B.; Veli, S. *J. Hazard. Mater.*, **2009**, *167*, 482-488.
9. Huang, Y.; Zeng, X.; Guo, L.; Lan, J.; Zhang, L.; Cao, D., *Separation and Purification Technology.*, **2018**, 462-469.
10. Sani, A.; Hussaini, K.; Sani, H. M., *Applied Water Science.,* **2017**, *7*, 3151–3155.
11. Mohamed, S.; Andrzej, G., *Acta Scientific Agriculture.,* **2020**, *4.2*, 01-10.
12. Gunjate, J.K. *IOSR-JESTFT.*, **2016**, *10*, 161-165.
13. Ojedokun, A.T.; Bello, O. S., *Water Resources and Industry.*, **2016**, 7-13.
14. Demirbas, A. *Journal of hazardous materials.*, **2008**, *157*, 220-229.
15. Berihun, D. *Journal of Materials Science and Engineering.*, **2017**, *6*(2), 6–11.
16. Bayuo, J.; Bayuo, K. B.; Pelig-ba, K. B.; Abukari, M. A. *Applied Water Science.*, **2019**, *9*(4), 1–11.
17. Bayuo, J.; Abukari, M. A.; Pelig-ba, K. B. *Journal of Applied Chemistry.*, **2018**, *11*, 40–46.
18. Gautam, A. K.; Markandeya, N.; Singh, B.; Shukla, S. P; Mohan, D. *SN Applied Sciences.*, **2020**, *2*(2), 1–11.
19. Grégorio, C.; Eric, L. *Environmental Chemistry Letters.*, **2019**, *17*(1), 145-155.
20. Gunjate, J. K.; Meshram, Y. K.; Khope, R.U.; Awachat, R. S. *Materials Today: Proceedings.*, **2020**, *29*, 1150–1155.
21. Furniss, B. S.; Hannaford, A. J.; Smith, P.W.G.; Tatchell, A. R. Vogel's Textbook of Practical Organic Chemistry. Pearson Education Ltd. **2012**, 1348.
22. Langmuir, I. Part I. Solids. *Journal of the American Chemical Society.*, **1916**, *38*(11), 2221-2295.
23. Freundlich, H. M. Over the adsorption in solution. *J. Phys. Chem.*, **1906**, *57*, 385-471.
24. Temkin, M. I.; Pyzhev, V. Kinetics of ammonia synthesis on promoted iron catalyst. *Acta Phys. Chim.*, **1940**, *12*, 32